Electron correlations in thin disordered quantum wires

J. S. Thakur
School of Physics, The University of New South Wales, Sydney 2052, Australia

D. Neilson
School of Physics, The University of New South Wales, Sydney 2052, Australia
and Scuola Normale Superiore, Piazza dei Cavalieri 7, 56126 Pisa, Italy
(Received 10 May 1996; revised manuscript received 15 August 1996)

We calculate self-consistently the dependence of electron-electron correlations on electron-defect scattering processes in quantum wires with only the lowest subband occupied. We use the Singwi-Tosi-Land-Sjölander approach to calculate the many-body electron-electron correlations. The effect of electron scattering from randomly distributed Coulombic impurities and off surface roughness of the wire is treated using self-consistent current-relaxation theory. Electron correlations can become very strong even at relatively high electron densities if the wire diameter is made sufficiently small. For a fixed disorder level the electron-defect scattering rate increases with increasing electron correlations. The plasmon dispersion depends on electron correlations and on the level of disorder. Electron-electron correlations transfer spectral weight at finite wave number from the plasmon to the single-particle excitations. [S0163-1829(97)04731-0]

Thin conducting wires fabricated using direct molecular beam epitaxy (MBE) growth on GaAs-AlAs tilted superlattices[1] are imperfect one-dimensional conductors. Imperfections come from the impurities embedded in the wire and surroundings as well as spatial variations of the wire diameter.

For noninteracting electrons in a wire with defects all the electron states are localized.[2] For interacting electrons in a wire with one subband and without disorder a Luttinger liquid picture is applicable. In real quantum wires with both electron-electron interactions and disorder, Fermi-liquid-like behavior may be restored if the localization length becomes larger than the physical length of the wire.[3,4] The presence of additional subbands, even if only negligibly occupied, can also help to restore Fermi-liquid-like behavior.

In this paper we work with realistic wires that have both impurities and surface roughness, and we look at the mutual dependence of electron-electron correlations and electron-defect scattering. We are particularly interested in the case where the electron correlations are strong. We adopt an approach that self-consistently combines the Singi-Tosi-Land-Sjölander (STLS) method[5] with a memory function calculation. The STLS is used for the electron correlations and the memory function is used to calculate the decay time of density fluctuations when they scatter off defects.

Recently Hu and Das Sarma[3] investigated the effect of ionized impurity scattering and finite temperatures on the electron self-energy and spectral function in a wire of finite diameter using the random-phase approximation (RPA). The effect of impurity scattering was treated by introducing an adjustable parameter γ representing the static defect scattering rate. They concluded that small levels of impurity scattering in a real sample would restore the Fermi surface and Landau Fermi liquid behavior to the system.

Li, Das Sarma, and Joynt[6] have shown at relatively high density and thick wire diameter, $r_s=0.8$ and $D/a_0^\star=3.1$, that the dispersion of the RPA plasmon and the dispersion calculated within the Luttinger-Tomonaga model are essentially identical for small momentum transfers $q/k_F \lesssim 0.2$. Dzyaloshinskii and Larkin[7] discussed correlation functions for the Tomonaga model for a one-dimensional Fermi system with long-range interactions. They established that the RPA is exact for small-q correlation functions where there is no backscattering. Their argument, however, does not apply to the large-q part of a physical density operator. The vertex corrections do not vanish for the $q=2k_F$ or $4k_F$ correlation functions of a physical density operator. In the presence of defects this argument cannot be applied even for small momentum transfers due to the backscattering introduced by the defects.

In STLS the static electron correlations are taken into account by replacing the Coulomb interaction by an effective interaction. This construction ensures that the f-sum rule is exactly satisfied in the STLS (Ref. 8) as it is in RPA. In the limits of high density or small momentum transfer, where the RPA is known to be exact, STLS goes continuously over to the RPA.

Friesen and Bergersen[9] used STLS to calculate the pair correlation function and the effect of correlations on the plasmon dispersion in a perfect quantum wire. They took an interaction of the form $V(q)=e^2E_1[(bq)^2]\exp[(bq)^2]\epsilon^{-1}$, where b is the decay length of a Gaussian wave function perpendicular to the wire, ϵ is the wire dielectric constant, and $E_1(x)$ is the exponential integral function. For small separations in real space this potential is the interaction between parallel planar charge distributions. Borges, Degani, and Hipolito[10] and Campos, Degani, and Hipolito[11] have investigated the plasmon excitation spectra using STLS for quasi-one-dimensional quantum-well wires. They calculated the pair correlation function as a function of wire thickness and electron density. References 9–11 neglect the effect of defects and are mainly concerned with electron densities and wire diameters such that the electron correlations are not very strong.

We investigate self-consistently the effect on the electron correlations of (i) charged impurities, (ii) the finite diameter of the wire, and (iii) spatial variations in the wire diameter (surface roughness scattering). The wire is treated as an infinite height well of width D with dielectric constant ϵ. A linear density n_i of randomly distributed Coulombic impurities of charge Ze is embedded in the wire. Electrons of linear density n and effective mass $m^\star$ are delocalized along the wire. Their average spacing is $r_s=(2na_0^\star)^{-1}$ in units of the effective Bohr radius $a_0^\star=(\epsilon\hbar^2)/(m^\star e^2)$. In GaAs $a_0^\star=9.8$ nm.

In our calculations the electron densities we considered ranged from a maximum of $r_s=1$ (corresponding in GaAs to $n=5\times10^5$ cm^{-1}), where we took wire diameters $0.1\lesssim D\lesssim 13$ nm, to a minimum of $r_s=10$ (corresponding to $n=5\times10^4$ cm^{-1}), where we took wire diameters $13\lesssim D\lesssim 127$ nm. Experiments are typically carried out with wires of diameters $D\lesssim 10$ nm and densities $n\lesssim 5\times10^5$ cm^{-1}. For such systems we confirm the electron correlations are weak. Our results provide a compelling motivation to develop experiments to cover the strongly correlated region. They demonstrate that strong correlations lead to measurable effects in the properties of the plasmon collective excitations.

Perpendicular to the wire the electrons occupy discrete subbands of energy $E_\nu=\pi^2\hbar^2\nu^2/(2m^\star D^2)$, with $\nu=1,2,3,\ldots$. Our calculations are at zero temperature and we consider densities where only the lowest-energy subband is appreciably occupied. The presence of these higher subbands can restore the Fermi-liquid picture. We find that the STLS results for the lowest subband under these conditions are insensitive to the existence of the higher subbands.

Within the RPA the dynamic response function is

$$\chi(q,\omega)=\frac{\chi^{(0)}(q,\omega)}{1+V(q)\chi^{(0)}(q,\omega)}, \tag{1}$$

where $\chi^{(0)}(q,\omega)$ is the dynamical susceptibility for free electrons in one dimension,[12,13]

$$\chi^0(q,\omega)=-\frac{k_F}{2E_F}\frac{1}{\pi q}\ln\left|\frac{(\omega)^2-(q^2-2q)^2}{(\omega)^2-(q^2+2q)^2}\right|. \tag{2}$$

Our $V(q)=2e^2K_0(qD)\epsilon^{-1}$ is the bare Coulomb interaction in the wire. $K_0(qD)$ is the zeroth-order modified Bessel function of the second kind. It diverges logarithmically for vanishing D, thus making $V(q)$ particularly sensitive to the thickness of the wire so that we can vary the strength of the electron correlations not only by changing the electron density but also by changing D.

To treat the correlations between the electrons the bare Coulomb interaction $V(q)$ is replaced by an effective interaction $V_{\rm eff}=V(q)[1-G(q)]$, where $G(q)$ is a static local field $G(q)$.[5] Because the electrons repel each other the effective interaction is generally less than $V(q)$. The response function is then

$$\chi(q,\omega)=\frac{\chi^{(0)}(q,\omega)}{1+V(q)[1-G(q)]\chi^{(0)}(q,\omega)}. \tag{3}$$

Disorder is introduced by replacing the free particle dynamical susceptibility $\chi^{(0)}(q,\omega)$ in Eq. (3) by $\chi^{(s)}(q,\omega)$.[14] This accounts for electron scattering off the disorder by means of a static defect scattering rate γ,

$$\chi(q,\omega)=\frac{\chi^{(s)}(q,\omega)}{1+V(q)[1-G(q)]\chi^{(s)}(q,\omega)},$$

$$\chi^{(s)}(q,\omega)=\frac{\chi^{(0)}(q,\omega+i\gamma)}{1-[i\gamma/(\omega+i\gamma)][1-\chi^{(0)}(q,\omega+i\gamma)/\chi^{(0)}(q)]}. \tag{4}$$

γ is related to the electron mean free path by the expression $\ell=e/(m^\star\gamma)$. In the diffusive regime $\chi^{(s)}(q,\omega)$ takes the form

$$\lim_{\omega,q\to0}\chi^{(s)}(q,\omega)=\frac{2m^\star}{\pi k_F\hbar^2}\frac{\mathcal{D}q^2}{\mathcal{D}q^2+i\omega}, \tag{5}$$

where $\mathcal{D}=v_F^2/\gamma$ is the diffusion constant.

We relate γ to the disorder potential by using the memory function formalism with the mode coupling approximation[15] for the density relaxation function. Reference 15 calculated γ in the same way, but correlations between the electrons were neglected (except for exchange). The dependence of electron correlations on γ neglecting disorder was derived in this way in Ref. 16. Here we include both electron correlations and disorder in a single self-consistent scheme. Thus we define

$$i\gamma=\frac{1}{m^\star n}\sum_q q^2[\langle|U_{\rm imp}(q)|^2\rangle+\langle|W_{\rm surf}(q)|^2\rangle]\times\left(\frac{\tilde\chi(q)}{\chi^{(0)}(q)}\right)^2\frac{\phi_0(q,i\gamma)}{1+i\gamma\phi_0(q,i\gamma)/\chi^{(0)}(q)}. \tag{6}$$

$\tilde\chi(q)=\chi^{(0)}(q)/\{1+V(q)[1-G(q)]\chi^{(0)}(q)\}$ is the static response function for correlated electrons. $\phi_0(q,i\gamma)=(1/i\gamma)[\chi^{(0)}(q,i\gamma)-\chi^{(0)}(q)]$ is the relaxation function for noninteracting electrons scattering from defects. $U_{\rm imp}(q)$ is the electron-impurity potential. With Coulombic impurities randomly distributed inside the wire, $\langle|U_{\rm imp}(q)|^2\rangle=n_i[(2Ze^2/\epsilon)K_0(qD)]^2$. We take the impurity charge $Z=1$. $W_{\rm surf}(q)$ accounts for surface roughness scattering.[17] We write $\langle|W_{\rm surf}(q)|^2\rangle=\sqrt{\pi}(dE_0/dD)^2\eta\delta^2\exp[-(q\eta/2)^2]$, where η and δ are surface roughness parameters and $E_0=5.76(a_0^\star/D)^2$ Ry*, is the lowest occupied subband energy level.

Our approach is different from that of Liu and Das Sarma.[18] They calculated the relaxation rate for free electrons scattering from impurities within the first Born approximation. In our method we consider correlated electrons scattering from both impurities and surface roughness.

In STLS we approximate the density-density correlation function by the nonlinear product, $\langle\delta\hat n(r,t)\delta\hat n(r',t)\rangle\approx\delta n(r,t)g(r-r')\delta n(r',t)$, where the $\delta n(r,t)$ are expectation values and $g(r)$ is the static electron-electron correlation function. This relation when combined with the Fourier relation between $g(r)$ and the static structure factor $S(q)$ gives an expression for the local field,

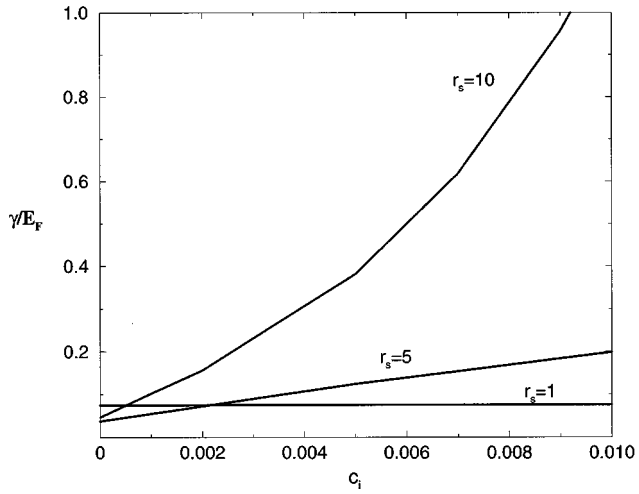

FIG. 1. Dependence of impurity scattering rate γ on impurity concentration c_i for different electron densities r_s as marked. Wire diameter is $D/a_0^\star = 2.6$. Surface roughness is fixed (see text).

$$G(q) = -\frac{1}{4qK_0(qD)}\int_0^\infty dk[(q-k)K_0((q-k)D) + (q+k)K_0((q+k)D)]\times[S(k)-1]. \quad (7)$$

γ depends on the local field $G(q)$ through $\tilde{\chi}(q)$ so $G(q)$ links the STLS equations and the expression for γ, Eq. (6). We use Eq. (4) together with the fluctuation-dissipation theorem to determine $G(q)$ through Eq. (7). With this $G(q)$ we solve Eq. (6) for γ. The new value of γ is substituted in Eq. (4) and the process is repeated until overall self-consistency is achieved.

The system parameters are (i) the electron density n, (ii) the wire diameter D, (iii) the density of randomly distributed impurities n_i, and (iv) the surface roughness. For our results here we fix the surface roughness parameters $\delta = 0.3$ nm and $\eta = 6$ nm, which are found for GaAs wires.[19,20]

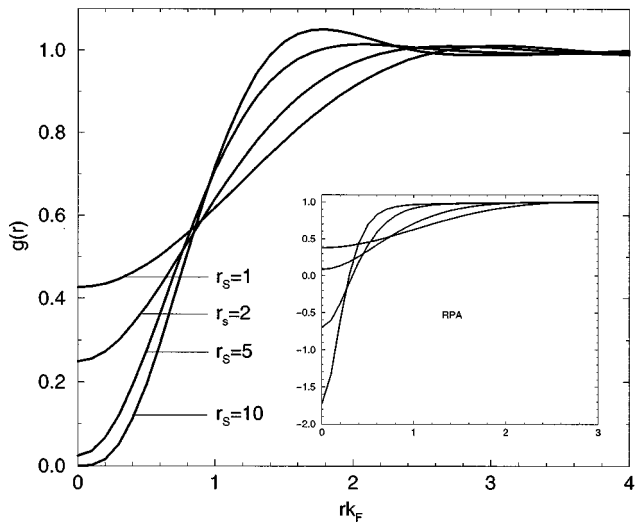

FIG. 2. Pair correlation functions $g(r)$ for different electron densities as marked. Wire diameter is $D/a_0^\star = 1.3$. Insets show the the corresponding $g(r)$ within the RPA.

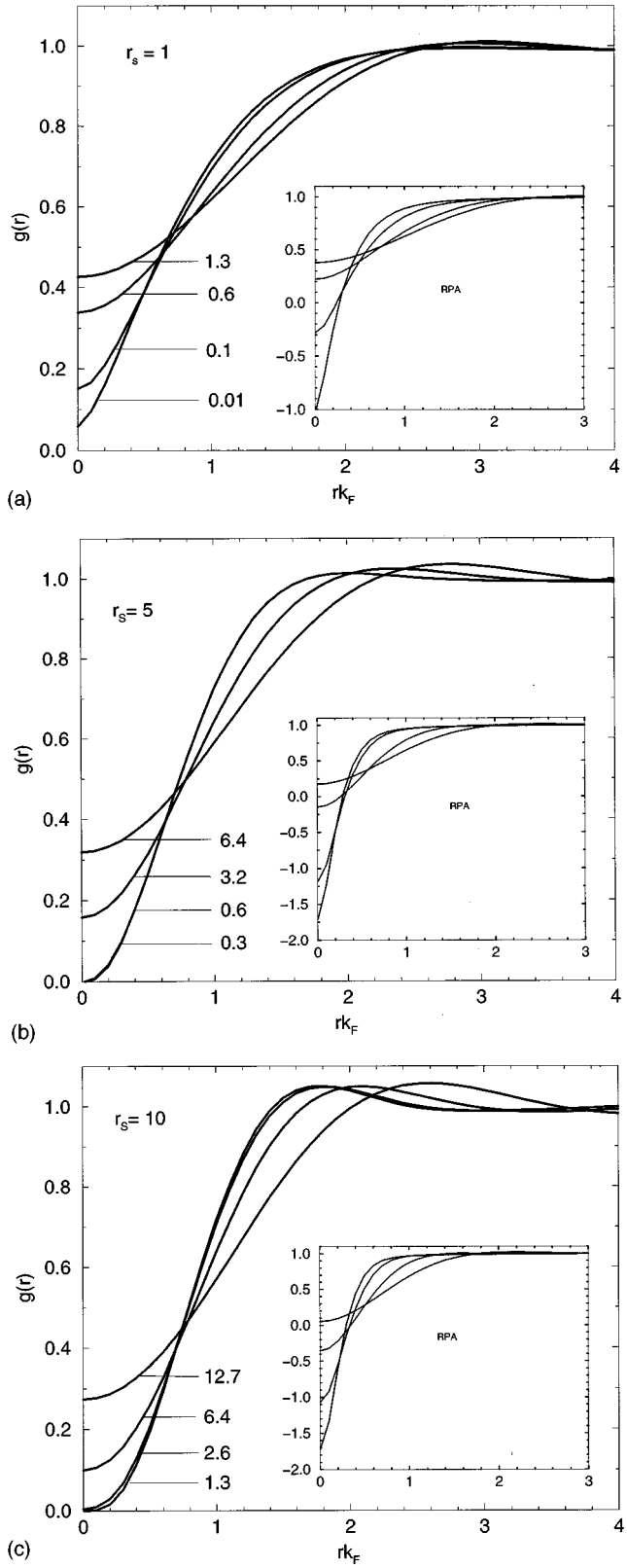

FIG. 3. Pair correlation functions $g(r)$ for different wire diameters D. Labels on curves indicate $D/a_0^\star$. The r_s for each panel is marked. Insets show the corresponding $g(r)$ within the RPA.

Figure 1 shows for different electron densities the dependence of γ on the normalized impurity density parameter $c_i = n_i/n$. For weak impurity scattering, that is, $\ell/r_0 = (8/\pi)(E_F/\gamma) \gg 1$, where r_0 is the average electron

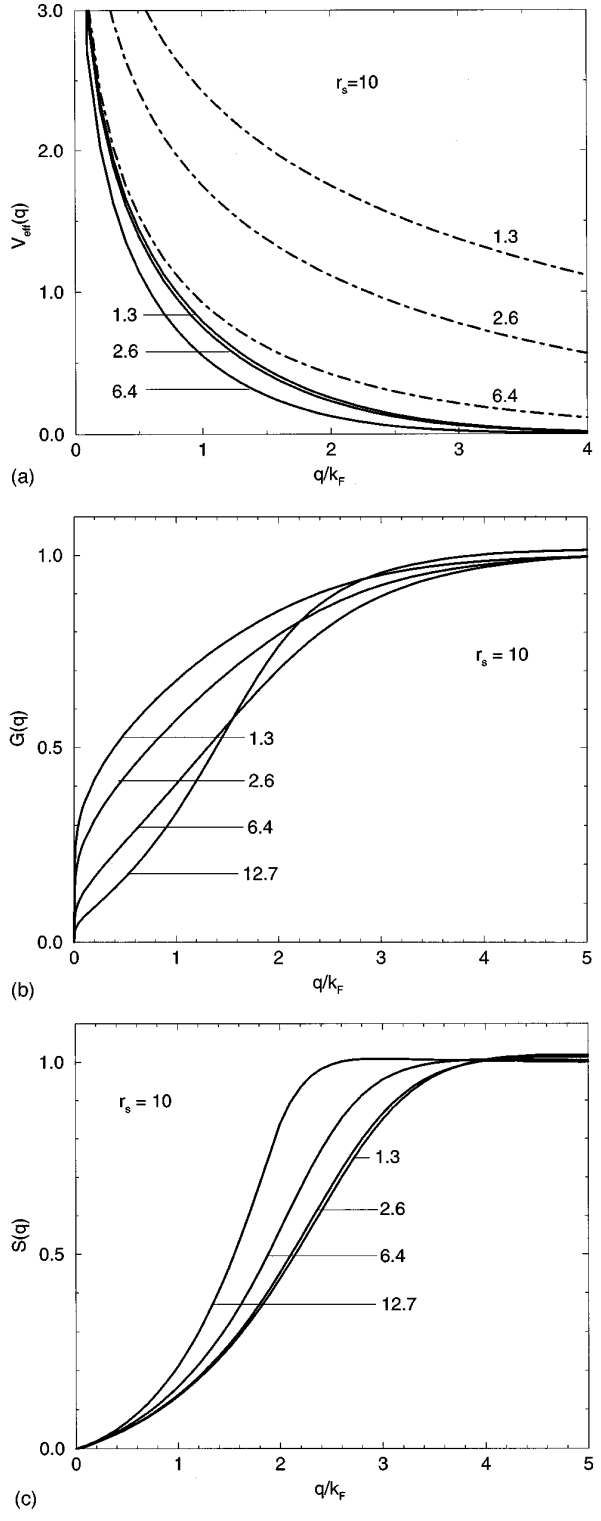

FIG. 4. In these panels electron density is $r_s=10$. Labels on curves indicate wire diameter $D/a_0^\star$. (a) Solid lines are the effective interactions $V_{\text{eff}}(q)$. Dotted lines are the corresponding bare Coulomb interactions $V(q)$. (b) Local fields $G(q)$. (c) Static structure factor $S(q)$.

spacing, the disorder concentration c_i is small and γ increases linearly with c_i.

We find that the static properties of the system are not sensitive to the presence of defects in the applicable range of $\gamma \lesssim E_F$. We present a single set of static results in the presence of impurities that are equally valid for all $\gamma < E_F$. In Fig. 2 the pair correlation function $g(r)$ is shown for densities $r_s=1$, 2, 5, and 10 for a fixed wire diameter $D/a_0^\star=1.3$. The inset shows the corresponding RPA results. We recall that the spin averaged $g_0(r)$ for the noninteracting system at $r=0$ equals 1/2. For $r_s=1$ the RPA and STLS produce similar results, indicating that correlation effects are small at this density. For $r_s>2$ the RPA $g(r)$ goes negative for small r. The corresponding STLS $g(r)$, however, remains positive. The discrepancy between the STLS $g(r)$ and the RPA $g(r)$ increases as the density is lowered, indicating that correlations are becoming stronger. The range of densities in Fig. 2 takes us from a regime where $g(r)$ approximates the noninteracting $g_0(r)$ to a $g(r)$ typical for a strongly interacting system. Thus at $r_s=10$ we see a total exclusion of electron density around each electron out to a separation $rk_F \simeq 0.1$ and a peak in $g(r)$ centered at $rk_F \simeq 1.8$.

In Fig. 3 we show the dependence of $g(r)$ on the wire diameter D for electron densities $r_s=1$, 5, and 10. The insets

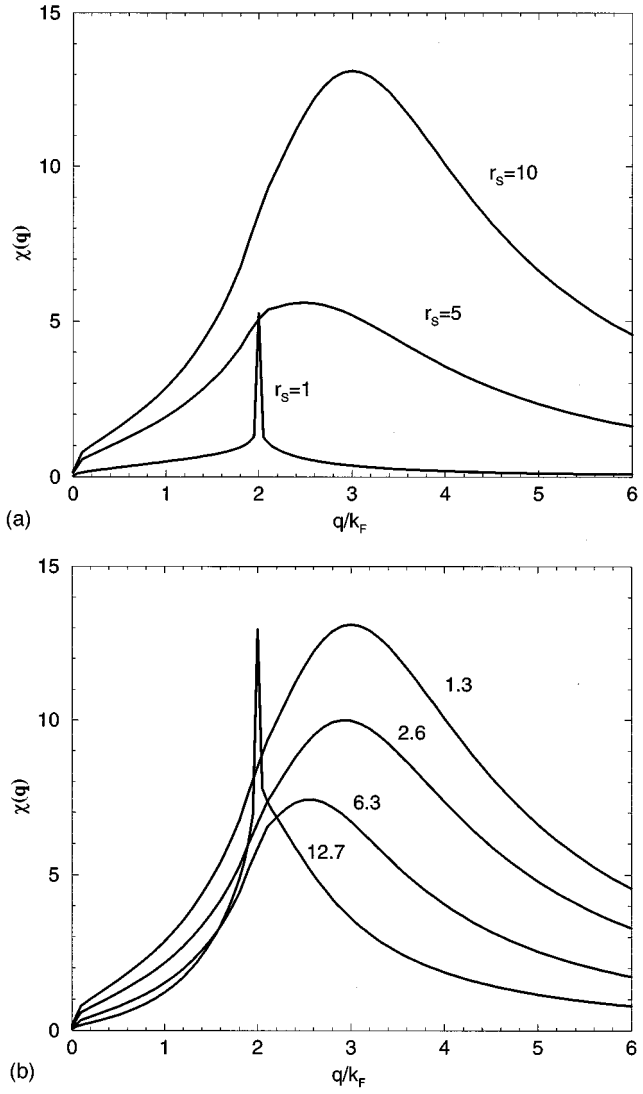

FIG. 5. (a) Static response function $V(k_F)\chi(q)$ for different electron densities r_s as marked. Wire diameter is $D/a_0^\star=1.3$. (b) $V(k_F)\chi(q)$ for $r_s=10$. Labels on curves indicate the different wire diameters $D/a_0^\star$.

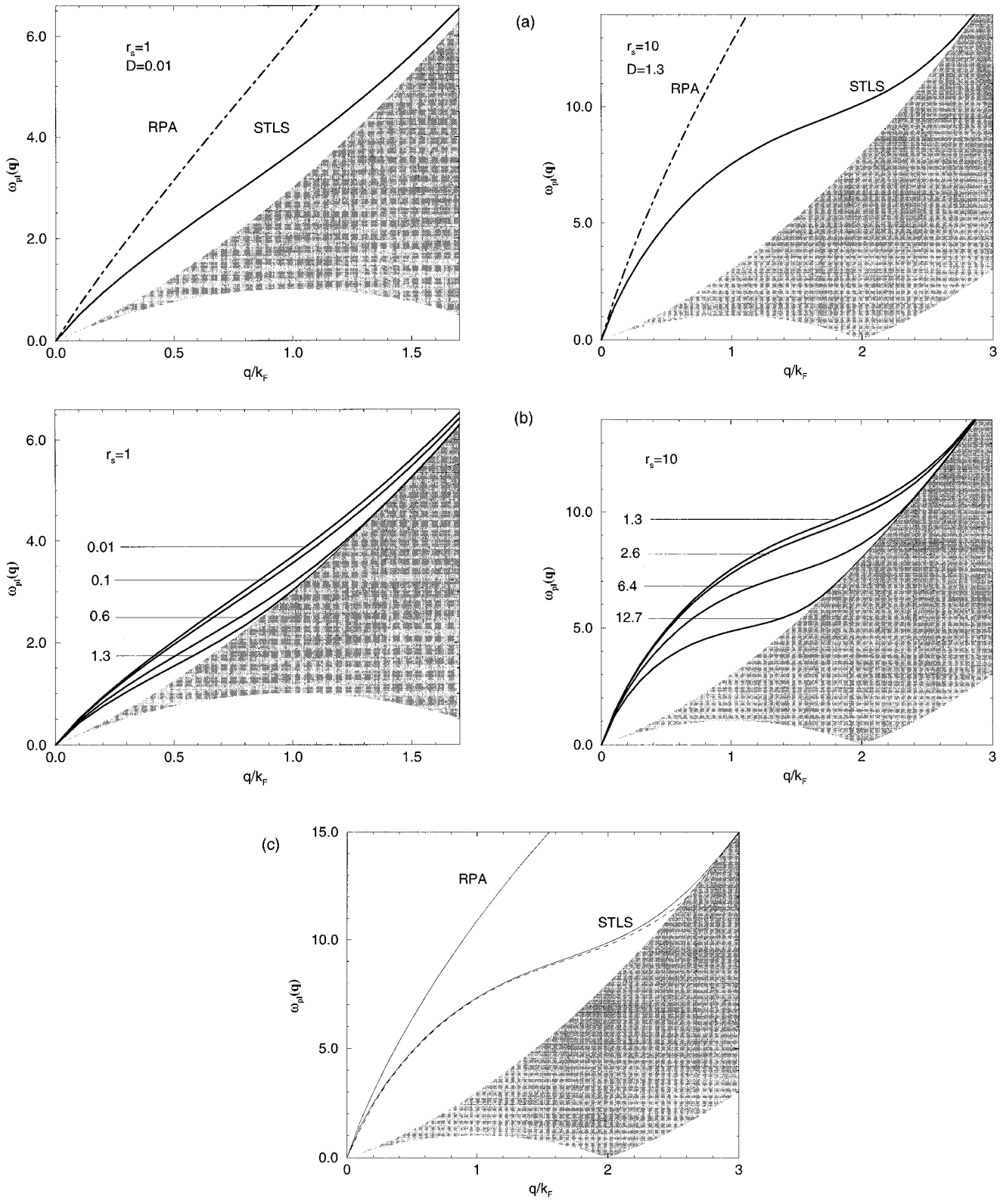

FIG. 6. Dispersion curves for the plasmon $\omega_{\rm pl}(q)$ with impurities and surface roughness (see text). Shaded areas are the single-particle excitation regions. (a) Without disorder. Electron density r_s and wire diameter $D/a_0^\star$ are marked on each panel. The solid line is from the present calculation. The dash-dotted line is the RPA. (b) Without disorder. Curves for different wire diameters $D/a_0^\star$ as marked. (c) Comparison with and without disorder. Electron density is $r_s=10$. Wire diameter is $D/a_0^\star=2.6$. Present calculation (STLS) and RPA curves as marked. Dashed lines: $c_i=0.01$ with surface roughness. Solid lines: without disorder.

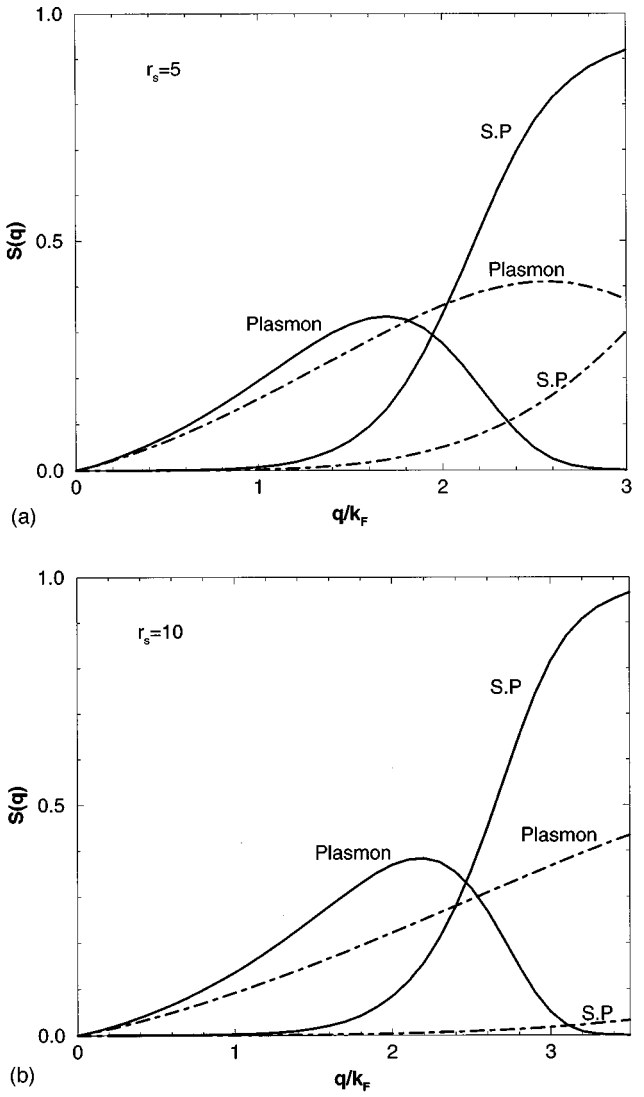

FIG. 7. Separate contributions to the static structure factor $S(q)$ from the plasmon and from single particle (S.P.) excitations (solid lines). The dotted lines are the corresponding contributions calculated within the RPA. Electron densities are as marked. The wire diameter is $D/a_0^\star = 2.6$.

show $g(r)$ calculated within the RPA for the same wire diameters. In the RPA the sensitivity of $g(r)$ to D is due solely to the increased strength of the bare Coulomb potential as D is decreased but in the full calculation this is compensated by the buildup in electron correlations [see Fig. 4(a)]. The net result is that our $g(r)$ is less sensitive to D than it is in the RPA and for $r_s = 5$ and 10 when D has become small $g(r)$ changes only slowly with D. For $r_s = 1$ $g(r)$ goes from the noninteracting result for larger D, to a quite strongly correlated system for smaller D.

We note in the RPA for $r_s = 1$ that $g(r)$ at small r goes negative for wire diameters $D/a_0^\star \lesssim 0.1$. A negative value for this positive definite probability function indicates a breakdown in the RPA. The breakdown occurs at increasingly larger values of D as r_s is increased.

For $r_s = 10$ our $g(r)$ has a peak. As D decreases the peak moves towards smaller r and at the same time the slope of $g(r)$ to the left of the peak becomes steeper. The maximum peak height does not increase with D.

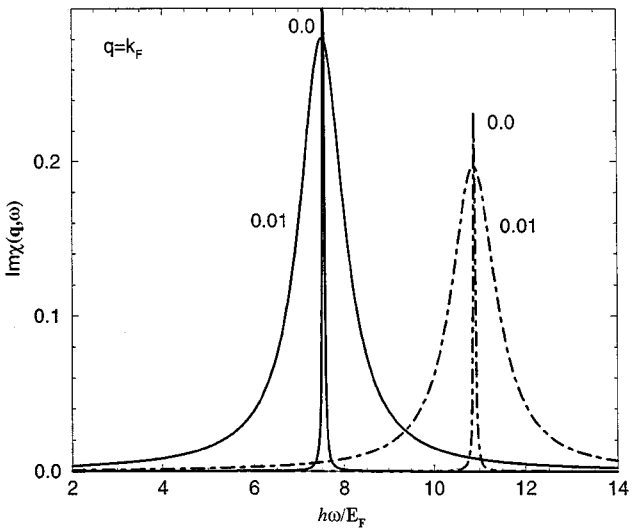

FIG. 8. $\mathrm{Im}\chi(q,\omega)$ for fixed $q/k_F = 1$ for wires with impurities and surface roughness. Electron density $r_s = 10$. Wire diameter is $D/a_0^\star = 1.3$. Labels on curves indicate impurity concentration c_i. The $c_i = 0$ peaks have been multiplied by a factor of 0.05. Solid lines are from present calculation. Dashed lines are RPA.

Figure 4(a) compares the effective interaction $V_{\mathrm{eff}}(q) = V(q)[1 - G(q)]$ at $r_s = 10$ with the bare Coulomb interaction $V(q)$ for three wire diameters D. For $D/a_0^\star \lesssim 2.6$ the changes in $G(q)$ compensate the dependence of $V(q)$ on D so that $V_{\mathrm{eff}}(q)$ is much more weakly dependent on D than is $V(q)$. The compensating changes is $G(q)$ are shown in Fig. 4(b). For smaller D the $G(q)$ increases more rapidly with q, indicating that the correlations are stronger. The range of q over which correlations have a significant effect on $\chi(q,\omega)$ decreases with increasing D and this explains for $D/a_0^\star \lesssim 12.7$ the more rapid increase of $G(q)$ towards unity in the range $q/k_F \gtrsim 1$.

The strong dependence of the correlations on wire diameter is again apparent in Fig. 4(c), which shows the static structure factor $S(q)$. However, even for the smallest wire diameter there is no indication of a peak in $S(q)$.

In Fig. 5(a) the static response function $\chi(q) = \chi(q,\omega=0)$ is shown at densities $r_s = 1$, 5, and 10 for a wire diameter $D/a_0^\star = 1.3$. Within the RPA $\chi(q)$ has a cusp at $q/k_F = 2$ that is a remnant of the cusp in the free-electron static susceptibility $\chi^{(0)}(q)$. For $r_s = 1$ where the correlations are weak the peak in $\chi(q)$ is still centered on $q/k_F = 2$ but as r_s increases the peak center moves towards larger q. By $r_s = 10$ it is centered on $q/k_F \simeq 3$. The peak height increases with r_s and it also broadens. We found no tendency for the peak to diverge.

Figure 5(b) shows the dependence of the static response function on wire diameter. The density is fixed at $r_s = 10$. For larger wire diameters, $D/a_0^\star \gtrsim 12.7$, where the correlations are weak the peak remains centered on $q/k_F = 2$. By the smallest wire diameter $D/a_0^\star = 1.3$ the center has moved to $q/k_F \simeq 3$.

We now turn to the dependence of the dynamical properties of the system on disorder. In the absence of disorder the plasmon dispersion $\omega_{\mathrm{pl}}(q)$ is determined from the zeroes in the denominator of Eq. (3). The analytical expression for $\omega_{\mathrm{pl}}(q)$ is

$$\omega_{\rm pl}(q)=2q\left[1+\frac{q^2}{4}+q\coth\left\{\frac{q\pi^2}{16r_sK_0(qD)[1-G(q)]}\right\}\right]^{1/2}. \tag{8}$$

In the RPA $\omega_{\rm pl}(q)$ merges with the single-particle excitation region in the asymptotic limit $q\to\infty$. The introduction of $G(q)$ lowers this cutoff wave vector, which is then determined by the q value at which $G(q)$ crosses unity. As r_s increases the value for the cutoff wave vector decreases.

In Fig. 6(a) our plasmon dispersion curves $\omega_{\rm pl}(q)$ are shown in the defect-free case (i) for electron density $r_s=1$ and wire diameter $D/a_0^\star=0.01$, and (ii) for electron density $r_s=10$ and wire diameter $D/a_0^\star=1.3$. The corresponding curves calculated within the RPA are also shown. The correlations introduced through the local field $G(q)$ weaken the effective electron-electron interaction and dramatically decrease $\omega_{\rm pl}(q)$ compared with the RPA. Even for a relatively high density $r_s=1$, strong electron correlations significantly depress the plasmon energy for small wire diameters.

Figure 6(b) shows $\omega_{\rm pl}(q)$ for $r_s=1$ and 10 for a range of wire diameters D. The variation in $\omega_{\rm pl}(q)$ with changing wire diameter is due (i) to the dependence of the Coulomb interaction on D and (ii) the dependence of $G(q)$ on D. The decrease of $\omega_{\rm pl}(q)$ with increasing D means that the dependence of $V(q)$ on D is the dominating effect. The results in Fig. 6 extend those of Refs. 11 and 13 into the region of strong electron correlations. For $r_s=10$ the local field $G(q)$ flattens $\omega_{\rm pl}(q)$ when $q/k_F\gtrsim 0.5$. For $r_s=1$ and large wire diameters the deviation from RPA is small. Thus the results reported by Goñi *et al.*[21] which are for $r_s=0.8$ and $D/a^\star=3$, are not affected by correlations.

Figure 6(c) shows the effect of impurities on the plasmon dispersion curve. $\omega_{\rm pl}(q)$ at finite c_i is determined from the peak position of $\mathrm{Im}\chi(q,\omega)$. Impurities depress $\omega_{\rm pl}(q)$ and reduce its curvature near the plasmon cutoff. The corresponding results in the RPA are also shown. The RPA curves are not sensitive to the presence of these impurities. We can estimate the localization length using the expression $\ell/r_0=(8/\pi)(E_F/\gamma)$. For $c_i\leqslant 0.01$ ℓ/r_0 remains much greater than unity so for these results we remain far away from localization.

In Fig. 7 we show in the absence of defects the separate contributions to the static structure factor $S(q)$ coming from the plasmon and from the single-particle excitations. The corresponding contributions calculated within the RPA are also shown. For $r_s=1$ STLS gives similar results to RPA. For $r_s\geqslant 2$ the single-particle excitations calculated within STLS are significantly greater than the RPA for a given value of q. For $r_s\geqslant 5$ the single-particle excitations start to be significant when $q/k_F\gtrsim 1.5$. After that the single-particle contribution increases rapidly with q. By $q/k_F\gtrsim 2-2.5$ these excitations have supplanted the plasmon as the dominant contributor to the spectral strength. The f-sum rule is automatically satisfied in the STLS (Ref. 8) as in the RPA. We found in our results that the numerical accuracy of the f-sum rule was the same in STLS as in RPA.

Figure 8 shows the variation with c_i of the imaginary part of the dynamic response function $\mathrm{Im}\chi(q,\omega)$ for fixed $q/k_F=1$. The wire diameter is $D/a_0^\star=1.3$ and the surface roughness is fixed. The dotted lines are the RPA result. For convenience the $c_i=0$ peaks have been multiplied by a scale factor of 0.05. Since we are at zero temperature the width of the peaks is determined by γ. For $c_i=0$ the finite width results from surface roughness scattering. As c_i increases the peaks broaden. The RPA peaks have almost the same width but are shifted towards higher frequencies.

In summary we developed a method to calculate self-consistently the interdependence between electron-electron correlations and the effects of electron scatterings off disorder. For the levels of disorder considered the properties of the system at lower electron densities or small wire diameters depend weakly on the disorder. Strong electron correlations significantly depress the dispersion curve of the plasmon and also significantly boost the spectral strength of the single-particle excitations so that the plasmon at finite q does not saturate the spectral strength.

We thank D. J. W. Geldart, G. La Rocca, M. P. Tosi, and J. Voit for helpful discussions. This work is supported by an Australian Research Council grant. D.N. thanks F. Bassani for the hospitality and facilities of the Scuola Normale Superiore.

[1] P. M. Petroff, J. Gaines, M. Tsuchiya, R. Simes, L. Coldren, H. Kroemer, J. English, and A. C. Gossard, J. Cryst. Growth **95**, 260 (1989).

[2] E. Abrahams, P. W. Anderson, P. A. Lee, and T. V. Ramakrishnan, Phys. Rev. Lett. **42**, 673 (1979).

[3] Ben Yu-Kuang Hu and S. Das Sarma, Phys. Rev. Lett. **68**, 1750 (1992); Phys. Rev. B **48**, 5469 (1993); **40**, 5860 (1989).

[4] S. Das Sarma and Wu-yan Lai, Phys. Rev. B **32**, 1401 (1985).

[5] K. S. Singwi, M. P. Tosi, R. H. Land, and A. Sjölander, Phys. Rev. **176**, 589 (1968).

[6] Q. P. Li, S. Das Sarma, and R. Joynt, Phys. Rev. B **45**, 13 713 (1992).

[7] I. E. Dzyaloshinskii and A. I. Larkin, Zh. Éksp. Teor. Fiz. **65**, 411 (1973) [Sov. Phys. JETP **38**, 202 (1974)].

[8] K. S. Singwi and M. P. Tosi, in *Solid State Physics*, edited by H. Ehrenreich, F. Seitz, and D. Turnbull (Academic, New York, 1981), Vol. 36, p. 177.

[9] W. I. Friesen and B. Bergersen, J. Phys. C **13**, 6627 (1980).

[10] A. N. Borges, M. H. Degani, and O. Hipolito, Superlattices Microstruct. **13**, 375 (1992).

[11] V. B. Campos, M. H. Degani, and O. Hipolito, Superlattices Microstruct. **17**, 85 (1995).

[12] P. F. Williams and Aaron N. Block, Phys. Rev. B **10**, 1097 (1974).

[13] Q. P. Li and S. Das Sarma, Phys. Rev. B **43**, 11 768 (1991); **40**, 5860 (1989).

[14] N. D. Mermin, Phys. Rev. B **1**, 2362 (1970).

[15] W. Götze, Solid State Commun. **27**, 1393 (1978); W. Götze, Philos. Mag. B **43**, 219 (1981); A. Gold and W. Götze, Solid State Commun. **47**, 627 (1983).

[16] D. Neilson, L. Świerkowski, A. Sjölander, and J. Szymánski, Phys. Rev. B **44**, 6291 (1991).
[17] A. Gold and A. Ghazali, Phys. Rev. B **41**, 7626 (1990).
[18] Dongzi Liu and S. Das Sarma, Phys. Rev. B **51**, 13 821 (1995).
[19] H. Sakaki, T. Noda, K. Hirakawa, M. Tanaka, and T. Matsusue, Appl. Phys. Lett. **51**, 1934 (1987).
[20] R. Gottinger, A. Gold, G. Abstreiter, G. Weimann, and W. Schlapp, Europhys. Lett. **6**, 183 (1988).
[21] A. R. Goñi, A. Pinczuk, J. S. Weiner, J. M. Calleja, B. S. Dennis, L. N. Pfeiffer, and K. W. West, Phys. Rev. Lett. **67**, 3298 (1991).